BOREAL ENVIRONMENT RESEARCH 12: 421–430 ISSN 1239-6095
Helsinki 25 June 2007 

# Simulating aerosol nucleation bursts in a coniferous forest

Hannes Tammet[1)] and Markku Kulmala[2)]

[1)] *Institute of Environmental Physics, University of Tartu, Ülikooli 18, 50090 Tartu, Estonia*
[2)] *Division of Atmospheric Sciences, Department of Physical Sciences, P.O. Box 64, FI-00014 University of Helsinki, Finland*

*Received 24 Sep. 2006, accepted 1 Feb. 2007 (Editor in charge of this article: Veli-Matti Kerminen)*

Tammet, H. & Kulmala, M. 2007: Simulating aerosol nucleation bursts in a coniferous forest. *Boreal Env. Res.* 12: 421–430.

We modified a numerical model of atmospheric aerosol nucleation bursts to include the dry deposition of ions and freshly nucleated particles onto tree needles in a coniferous forest. The dry deposition is estimated using the Churchill-Bernstein approximation, which is adapted from the theory of heat transfer. The model includes an improved submodel of the sink of ions and nucleation mode particles onto large particles of the background aerosol. The user can edit the values of 95 input parameters by altering a control file. The computing time on an ordinary PC is counted in seconds in case of a typical task, which is characterized by several thousands of time steps and several thousands of size sections. The numerical examples show that, during atmospheric aerosol nucleation events, the dry deposition of ions and nanometer scale particles onto the conifer needles has a considerable effect on the respective concentrations.

## Introduction

Research of the atmospheric aerosol nucleation bursts is an important source of information about the mechanisms that control the formation and growth of new particles in the Earth's atmosphere. An overview of problems and observations of the formation and growth of atmospheric aerosol particles is presented in a paper by Kulmala *et al*. (2004b). The observations of aerosol nucleation bursts are interpreted in terms of parameters of theoretical models, e.g. the nucleation rate and the particle growth rate. Fitting the parameters with the measurements is not a trivial task. Tammet and Kulmala (2005) created a computer program for simulating nucleation bursts. The user could control a large number of parameters of the theoretical model and the variation of different quantities was tabulated for comparison of the model with the measurements. The considered physical processes were ion-induced and homogeneous nucleation, depletion of nanoparticles and ions onto pre-existing aerosol particles, nano-Köhler growth function, molecule-particle interception geometry, quantum retardation of sticking, electric charges of particles, molecular dipole moments, and polarization interaction.

Long-term complex aerosol measurements are being performed in Hyytiälä, Finland, where a large number of nucleation events have been recorded in a coniferous forest (Dal Maso *et al*. 2005). Tammet *et al*. (2006) showed that dry deposition of air ions onto the conifer needles has a considerable effect on the air ion concentration in the forest. The dry deposition of the ions and freshly nucleated particles was not considered in the previous paper by Tammet and Kulmala (2005), and so the results cannot be

immediately used for the analysis of the measurements made in Hyytiälä. The model will be updated in the present study. The dry deposition onto the conifer needles will be included according to Tammet *et al*. (2006) by using the Churchill-Bernstein approximation, which is adapted from the theory of heat transfer. Additionally, the submodel of the sink of ions and nucleation mode particles onto large particles of the background aerosol will be improved.

The submodels of condensation, coagulation, depletion and growth of particles will be adapted without changes from Tammet and Kulmala (2005) and are not described in the present paper, which is written as an extension of the previous study.

## General conventions

Most of the general conventions, presumptions and simplifications made here are the same as in Tammet and Kulmala (2005). Particles in the air are classified as molecules, Van der Waals clusters, macroscopic particles and ions. Clusters and particles are distinguished according to their electron structure and the separation of internal energy levels. The diameter at which the separation of energy levels matches the average thermal energy is estimated to be about 1.6 nm when fitting the measured mobilities of ions (Tammet 1995). The size of a particle is characterized by its mass diameter $d_p$ given by

$$d_p = \sqrt[3]{\frac{6m}{\pi\rho}}, \qquad (1)$$

where $m$ is the mass of the particle and the density of the particulate matter, $\rho$, is expected independent of the particle size.

The particles are divided into two classes: fresh particles born during the nucleation burst and pre-existing background aerosol particles. The fresh particles are expected to grow in the nanometer size range and the background aerosol particles are expected to be bigger than the largest fresh particles. The mechanism of nucleation is not discussed and the nucleation rates are defined separately for the neutral, positive and negative particles as the input parameters of the model. The nucleation rates are presented as "real" rates, which differ from the "apparent" rates as explained by Kerminen and Kulmala (2002). The fresh particles are assumed to be neutral or singly charged. These particles can grow, recharge with encountered ions and deplete onto the pre-existing aerosol particles or canopy. The mutual coagulation of fresh particles is neglected. This simplification may limit the applications to weak and moderate bursts of nucleation. Traditionally, the growth of aerosol particles is considered by condensation of vapor molecules. The size of some condensing molecules can be too large to be neglected and the added substance may consist of clusters, which are expected to be always present in the atmosphere (Kulmala *et al*. 2000). Thus, the growth of particles is considered as a combination of particles with growth units of finite size, which may be molecules or clusters of molecules. The term "growth units" is adopted from the physics of crystal growth. Two kinds of growth units are considered in the model. Substances of the first kind of growth units are responsible for the nucleation and slow initial growth of particles. Evaporation these substances is neglected. Substances of the second kind of the growth unit may evaporate and be responsible for quicker growth after the particles have passed the threshold size of the nano-Köhler model (Kulmala *et al*. 2004a). The coagulation of particles and growth units is described using the Sahni interpolation (Fuchs and Sutugin 1971, Tammet and Kulmala 2005) between the free molecule and continuum regimes. The attachment of ions to particles is considered according to an approximation of the numerical results by Hoppel and Frick (1986) and measurements by Reischl *et al*. (1996). Interaction with the induced dipole moments of growth units is included according to (∞–4) potential model (Tammet 1995). Two alternative methods of accounting for the interaction of charged particles with the polar molecules like sulfuric acid are considered. The first method uses the concept of total effective polarizability and the second method uses the results by Nadykto and Yu (2003). The ion and particle size-mobility relation and the Van der Waals capture distance are calculated according to the model by Tammet (1995). The dry deposition of ions and nanometer particles in a coniferous

forest is described using the Churchill-Bernstein approximation (Tammet *et al*. 2006).

The initial situation before the nucleation burst is described by user-controlled constants and functions. The predetermined constants include the temperature, air pressure, mobilities of positive and negative ions, mutual recombination coefficient of ions, density of ionic matter, density of growth units and particulate matter, diameters of growth units, birth size of particles, threshold of the nano-Köhler growth, capture distance of the Van der Waals force, polarizabilities or effective polarizabilities of growth units, critical size and extra temperature of quantum retardation of sticking, and relations of positive and negative nucleation rates to the neutral nucleation rate. The parameters of nucleation can be described with different numbers for the free air and the forest canopy. The predetermined functions describe the time variations of ionization rate and nucleation rate, the concentration and average diameter of pre-existing aerosol particles, and the plain Knudsen growth rates defined as the limits of growth rates for sticky neutral sizeless growth units. The parameters of the model are presented in a control file and can be edited using a plain text editor.

## Equations of the evolution and balance of ions

The source of ions is the ionizing radiation characterized by the ionization rate $I$. The sinks of ions include ion-induced nucleation characterized by the rates $J^+$ and $J^-$, mutual recombination, attachment to aerosol particles, and dry deposition onto the canopy. The last factor is important for forest measurement stations. The equations of evolution for the positive and negative ion concentrations $n^+$ and $n^-$ are

$$\left.\begin{aligned}\frac{dn^+}{dt} &= I - J^+ - (s_i^+ + s_n^+ + s_b^+ + s_f^+)n^+ \\ \frac{dn^-}{dt} &= I - J^- - (s_i^- + s_n^- + s_b^- + s_f^-)n^-\end{aligned}\right\}, \quad (2)$$

where $s_i$ is the sink of ions on the cluster ions of opposite polarity, $s_n$ is the sink of ions on the nucleation mode particles, $s_b$ is the sink of ions onto the background aerosol, and $s_f$ is the sink of ions onto the forest canopy; $s$ is used to mark the sinks of cluster ions, whereas $S$ is reserved for the sinks of freshly-nucleated nanometer particles. The mutual recombination sinks of cluster ions depend on the recombination coefficient $\alpha$:

$$\left.\begin{aligned}s_i^+ &= \alpha n^- \\ s_i^- &= \alpha n^+\end{aligned}\right\}, \quad (3)$$

The sink of cluster ions onto aerosol particles is calculated as an integral over the particle size distribution and divided into two components, $s_n$ and $s_b$, because nucleation mode particles and background aerosol particles are separately considered in the model. The sink onto the nucleation mode aerosol particles is calculated according to the model by Tammet and Kulmala (2005). The model of the sink onto the background aerosol is improved, as will be explained in the following section of the paper.

In a steady-state situation the derivatives of ion concentrations in Eq. 2 are zero and the equations may be numerically solved to obtain the steady-state concentrations of ions. An explicit algebraic solution is not possible because the aerosol sinks $s_n$ and $s_b$ depend on the concentrations of ions.

## Depletion of ions on large particles of the background aerosol

Tammet and Kulmala (2005) calculated the sinks of ions on the background aerosol by means of an approximation

$$\left.\begin{aligned}s_b^+ &= 2\pi D^+ \left(d_p - q_p d_q\right) N_b \\ s_b^- &= 2\pi D^- \left(d_p + q_p d_q\right) N_b\end{aligned}\right\}. \quad (4)$$

Here $D^+$ and $D^-$ are the diffusion coefficients of ions, $N_{nb}$ is the concentration of pre-existing particles of the background aerosol, $d_p$ and $q_p$ are the mean diameter and algebraic mean charge number of aerosol particles, respectively, and $d_q$ is the characteristic length of Coulomb attachment given by

$$d_q = \frac{e^2}{4\pi\varepsilon_0 kT} \approx 1.671\times10^4 \Big/ T\,(\mathrm{nm}). \quad (5)$$

Here $e$ is the elementary charge, $\varepsilon_0$ is the electric constant, $k$ is the Boltzmann constant, and $T$ is the absolute temperature (K). The model is exact in the limit of large particles but the error in the size range of the accumulation mode is considerable. In the present study an improved approximation to $s_b$ is used

$$\left.\begin{aligned} s_b^+ &= 2\pi D^+ \left[(d_p - 1.5\ \text{nm}) - cq_p d_q\right] N_b \\ s_b^- &= 2\pi D^- \left[(d_p - 1.5\ \text{nm}) + cq_p d_q\right] N_b \end{aligned}\right\}, \quad (6)$$

where

$$c = \frac{d_p + 9\ \text{nm}}{d_p + 23\ \text{nm}} \quad (7)$$

is a size dependent correction coefficient.

The approximation given by Eq. 6 was proposed by Tammet *et al*. (2006), who also found the deviations from the exact model. They considered the steady state charge distribution of monodisperse particles to be controlled by the coefficient of unipolarity of the cluster ion polar conductivities and presumed that the charge distribution of the particles changes only due to the attachment of cluster ions. At first, the cluster ion sinks and particle mean charges were calculated according to the exact equations and then the approximate values of particle size and mean charge were restored by solving Eqs. 4 and 6. The errors of the simplified parametric models were characterized by relative deviations of restored values from the original values. The calculations showed that the use of the Eq. 4 for the accumulation mode particles is followed by relatively small errors of about a few percent in the estimated particle size, but considerable errors up to 30% in the estimated particle charge. The errors associated with the improved approximation (Eq. 6) did not exceed 5% in the particle size range of 10–1000 nm.

The aerosol sink is not exactly proportional to the particle size due to the nonlinear coefficient $c$ in Eq. 6. However, the deviation from the linearity is not large in the range of particle sizes dominating in the typical background aerosol, and the approximation given by Eq. 6 is applied to the polydisperse atmospheric aerosols considering $d_p$ equal to the mean diameter of background aerosol particles.

## Depletion of ions and nanometer scale particles on the forest

Deposition of cluster ions is a specific problem not considered in traditional models of dry deposition (*see* e.g. Seinfeld and Pandis 1998, Wesely and Hicks 2000). For gaseous species, reactivity is a major factor affecting the deposition velocity. In contrast to gases the cluster ions are fully adsorbed when reaching the surface of a conifer needle. The application of the models of dry deposition of particles in coniferous forests was described by Rannik *et al*. (2003). In contrast to the particles, the cluster ion deposition can be described using the methods of the theory of heat transfer (e.g. Incropera and Dewitt 2002). These methods allow developing a local model of cluster ion deposition onto individual needles (Tammet *et al*. 2001, 2006).

Needles make most of the adsorbing surface of trees in boreal forests (Chen *et al*. 1997). For the sake of simplicity only the needles are considered in the present model and the deposition onto trunks and branches of the trees is ignored. Unlike aerosol particles, the needles do not fly with the moving air, and thus the wind is an essential factor of the sink. The real orientation of conifer needles according to the wind is random. Deposition onto the needles, which are directed along the wind, is much less than deposition onto the transversal needles and can be neglected in the first approximation. In the first approximation, an inclined needle is considered as a composition of three Cartesian components, where one component is directed along the wind and two components are transversal to the wind. Thus two thirds of the needles are considered as cluster ion sinks in the present model and the orientation of these needles is assumed to be transversal to the wind.

A conifer needle is modeled as a segment of a thin and long cylinder. The heat flux and diffusion to a cylinder is described in terms of a local deposition velocity, $u_{dep}$, related to the longitudinal section of the cylinder: flux = $u_{dep}$ × (area of the longitudinal section). All needles in a volume unit have the total longitudinal section area of $L_n d_n$, where $L_n$ is the needle length density of the forest measured by the total length of needles in a volume unit, and $d_n$ is the average diameter of

needles. When two thirds of the needles are considered, the diffusion sink of cluster ions in the forest becomes equal to

$$s_f = \frac{2}{3} L_n d_n u_{dep}. \quad (8)$$

The local deposition velocity of air ions or nanometer particles from the transversal air flow related to the longitudinal section of a cylinder is expressed in terms of the Sherwood number Sh (Incropera and Dewitt 2002)

$$u_{dep} = \frac{D}{d_n} \mathrm{Sh}, \quad (9)$$

where $D$ is diffusion coefficient of ions or particles and $d_n$ is the diameter of the cylinder. Thus the forest sink of cluster ions is

$$s_f = \frac{2}{3} L_n D \, \mathrm{Sh}. \quad (10)$$

The amount of the adsorbing surfaces in a forest is usually characterized by the leaf area index. Different definitions of the index are used in the literature; (*see* Chen *et al*. 1997). The most unambiguous concept is the total or all-sided leaf area index $\mathrm{LAI_T}$, which is defined as the ratio of the total leaf or needle area in a vertical column of the forest to the cross-section area of the column. Thus $\mathrm{LAI_T} = \pi d_n L_n H$, where $L_n$ is presented as the average value over the full height of the forest $H$, and the average needle length density of forest canopy can be estimated as

$$L_n = \frac{\mathrm{LAI_T}}{\pi d_n H}. \quad (11)$$

The value of $L_n$ in a typical forest is of the same magnitude as the length of the chain of aerosol particles in a cubic meter $d_p N_b$. Thus the sink of cluster ions onto a forest canopy is expected to be of the same magnitude as the sink of cluster ions onto aerosol particles.

The value of the Sherwood number for a thin cylinder can be estimated according to the Churchill-Bernstein heat transfer equation (*see* Incropera and Dewitt 2002) translated into the terms of particle diffusion:

$$\mathrm{Sh} = 0.3 + \frac{0.62\,\mathrm{Re}^{1/2}\,\mathrm{Sc}^{1/3}}{\left[1+\left(0.4/\mathrm{Sc}\right)^{2/3}\right]^{1/4}} \left[1+\left(\frac{\mathrm{Re}}{282000}\right)^{5/8}\right]^{4/5}. \quad (12)$$

The Reynolds number Re and the Schmidt number Sc are defined as

$$\mathrm{Re} = \frac{u d_n}{\nu}, \; \mathrm{Sc} = \frac{\nu}{D}, \quad (13)$$

where $u$ is the wind speed and ν is the kinematic viscosity of air. The Sherwood number depends via the Schmidt number on the ion mobility and therefore the deposition velocity is not exactly proportional to the mobility.

The Churchill-Bernstein equation is adequate when $\mathrm{Re} \times \mathrm{Sc} > 0.2$ and cannot be used for still air. The wind speed should be at least 0.007 m s$^{-1}$ for cluster ions and 0.5 m s$^{-1}$ for 10 nm particles. The model is satisfactory because the deposition of larger particles in a coniferous forest is weak and can be ignored in the present study.

## Processing of a nucleation burst in the forest

The residence time of the air in a forest is typically less than the duration of a nucleation burst. The air package arriving at the measuring point is expected to be aged for an unlimited time in the free air space before entering into the forest, and for a few minutes before measurements inside the forest canopy. The residence time of air in forest may vary depending on the time evolution of the wind speed, as specified in the input data of the simulator. The time in the simulator output is counted from the beginning of the burst. The simulator calculates the air ion and aerosol particle distributions for a finite set of output moments, which can be interpreted as moments of measurements. When the forest is not considered, a single integrating process delivers step by step the results for all output moments. The forest complicates the task because environmental conditions are changed when air enters the forest. The processes for different output moments are illustrated in Fig. 1. The intermediate results of different processes coincide only for the left-hand parts of the bars when the air has not yet entered the forest. Inside the forest every process should be integrated independently. For the sake of simplicity, the diagram includes only six processes while a typical problem consists of a few tens of output moments.

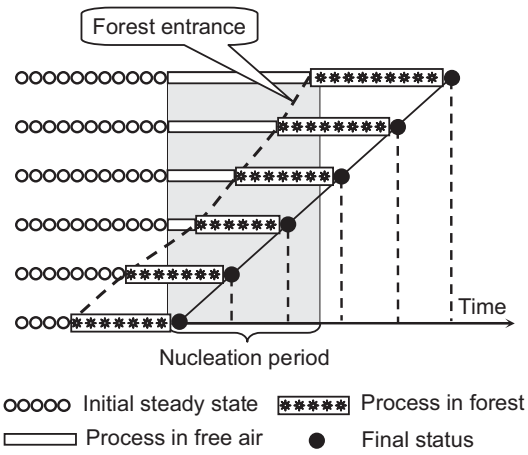


**Fig. 1**. Processing of a nucleation burst. Six processes are illustrated with six horizontal bars. Steady state is expected until the beginning of nucleation or until the entrance of the air into the forest. The crooked forest entrance line reflects the variations in the forest residence time in the example.

The distribution of freshly nucleated particles is described in a sectional model by the section concentrations $N_i$ corresponding to particle diameter sections ($d_{p,i-1}$ ... $d_{p,i}$). The number of sections is controlled by the user, a typical value being a few thousands. The growth of particles from the $i$th section to $(i + 1)$th section during a short time interval $\Delta t$ depends on the average value of the particle size distribution function and the particle growth rate.

The environmental situation and conditions of the nucleation burst are described in a file of control parameters. Most of environmental parameters can be presented with a parabolic trend. Several parameters, e.g. nucleation rate parameters, can be presented with two different numbers: one for the free air and the other for the forest canopy. The total number of parameters controlled by the control file is 95.

The algorithm includes five stages. At the first stage, the control file is analyzed and the values of the following quantities are calculated and tabulated in memory as functions of time for the full period under consideration:

— wind velocity and air residence time in the forest,
— background aerosol average diameter and concentration,
— ionization rate $I$ and nucleation rates $J^+$, $J^-$, $J^\circ$ for charged and neutral particles in free air and in the forest,
— ion sinks in forest $s^+_f$ and $s^-_f$ (Eqs. 10–13),
— particle sinks onto the background aerosol $S_{b,i}$ for all size sections $i$ using the method described by Tammet and Kulmala (2005),
— attachment coefficients of ions (first polarity index) to particles (second polarity index) $\beta^{+\circ}_i$, $\beta^{-\circ}_i$, $\beta^{+-}_i$, $\beta^{-+}_i$, for all particle size sections $i$,
— growth rates $G(d_{p,i})$ of neutral and charged particles for all sections $i$ in free air.

The concentrations of the nucleation mode particles $N_i$ in all sections are set to zero and the steady-state concentrations of the ions and the background aerosol charge are calculated according to Eqs. 2–7. At the end of the first stage the pre-burst state in free air indicated with empty circles in Fig. 1 is known.

The second stage covers the nucleation process in the free air depicted with empty bars in Fig. 1. The parallel processes defined for different output moments coincide until the air enters the forest. The integration technique is the same as explained by Tammet and Kulmala (2005). A typical number of steps is a few thousands. The ion sinks onto nanometer particles are recalculated in every step of the integration process. Growth transfers of particles from the section $i$ to the section $i + 1$ are calculated according to a simple and stable algorithm

$$\Delta N_{i\to i+1} = \frac{G(d_{p,i})\Delta t}{\Delta d_p} N_i. \qquad (14)$$

The simplified algorithm of an integration step is

$$\left.\begin{aligned}
\frac{\Delta n^+}{\Delta t} &= I - J^+ - \left(\alpha n^- + s_b^+ + s_f^+ + \sum \beta_i^{+\circ} N_i^\circ + \sum \beta_i^{+-} N_i^-\right) n^+ \\
\frac{\Delta n^-}{\Delta t} &= I - J^- - \left(\alpha n^- + s_b^- + s_f^- - \sum \beta_i^{-\circ} N_i^\circ + \sum \beta_i^{-+} N_i^+\right) n^- \\
\frac{\Delta N_i^+}{\Delta t} &= \delta_{1,i} J^+ + \left(1-\delta_{1,i}\right)\frac{\Delta N_{i-1\to i}^+}{\Delta t} - \frac{\Delta N_{i\to i+1}^+}{\Delta t} \\
&\quad + \beta_i^{+\circ} n^+ N_i^\circ - \left(\beta_i^{+-} n^- + S_{b,i} + S_{f,i}\right) N_i^+ \\
\frac{\Delta N_i^-}{\Delta t} &= \delta_{1,i} J^- + \left(1-\delta_{1,i}\right)\frac{\Delta N_{i-1\to i}^-}{\Delta t} - \frac{\Delta N_{i\to i+1}^-}{\Delta t} \\
&\quad + \beta_i^{-\circ} n^- N_i^\circ - \left(\beta_i^{+-} n^+ + S_{b,i} + S_{f,i}\right) N_i^- \\
\frac{\Delta N_i^\circ}{\Delta t} &= \delta_{1,i} J^\circ + \left(1-\delta_{1,i}\right)\frac{\Delta N_{i-1\to i}^\circ}{\Delta t} - \frac{\Delta N_{i\to i+1}^\circ}{\Delta t} \\
&\quad + \beta_i^{-+} n^- N_i^+ + \beta_i^{+-} n^+ N_i^- - \left(\beta_i^{+\circ} n^+ + \beta_i^{-\circ} n^- + S_{b,i} + S_{f,i}\right) N_i^\circ
\end{aligned}\right\}. \qquad (15)$$

Here $\delta_{1,i}$ is the Cronecker symbol that is equal to 1 if $i = 1$ and equal to 0 otherwise. Eq. 15 is written in the common form for the second and fourth stages of the algorithm and it formally includes the forest sinks of cluster ions ($s_f$) and nucleation mode particles ($S_f$). The forest sinks are expected to be zero during the second stage of the algorithm. At the end of the second stage the air ion and aerosol distributions on the line of forest entrance in Fig. 1 are known.

The third stage includes the preparative calculations for the optimization of the integration of air ion and aerosol dynamics in the forest. The growth rates of particles and sinks of particles onto the forest canopy ($S^+_{f,i}$, $S^-_{f,i}$ and $S°_{f,i}$) are tabulated for all size sections and time intervals. The precondition of Churchill-Bernstein equation $\mathrm{Re} \times \mathrm{Sc} > 0.2$ can be violated only for large particles whose loss onto needles is negligible. Thus the sinks of nucleation mode particles on the forest canopy ($S_f$) are calculated in the same way (Eqs. 10–13) as the forest sinks of cluster ions.

The fourth stage includes the evolution of air ion and aerosol particle distributions inside of the forest canopy. The evolution of air ions and nucleation mode particles is integrated according to Eq. 15 considering now the pre-calculated sinks of ions and particles on the forest canopy. The initial state of air ion and aerosol distribution in the fourth stage is specific for different processes and every process illustrated with a horizontal bar in Fig. 1 must be integrated individually during the residence time of the air in the forest canopy. At the end of the fourth stage, the air ion and aerosol distributions at the output moments are known.

In the fifth stage the export values are calculated using the data collected during the previous stages. The list of the export variables is specified in the control file and it may include the nucleation rates, concentrations of ions and particles, background aerosol charge, average sizes of neutral and charged nanometer particles in a prescribed size range or in the full size range, indices of charge asymmetry of particles, and particle size distribution tables.

The algorithm used in the computer program of the simulator differs from that explained above only in technical details and in some formal transformations that accelerate the calculations.

## Examples of simulating a nucleation burst

Figure 2 was created as an example according to the results of simulating a fictitious aerosol nucleation burst assuming mixed neutral and ion-induced nucleation in the following conditions:

- temperature: 0 °C,
- pressure: 1013 mb,
- ionization rate above and inside the forest: 3 $\mathrm{cm^{-3}\ s^{-1}}$ and 5 $\mathrm{cm^{-3}\ s^{-1}}$,
- mobilities of positive and negative ions: 1.36 and 1.56 $\mathrm{cm^2\ V^{-1}\ s^{-1}}$,
- recombination coefficient: $1.6 \times 10^{-6}$ $\mathrm{cm^3\ s^{-1}}$,
- density of ions: 2 $\mathrm{g\ cm^{-3}}$,
- birth size of particles: 1.5 nm,
- neutral nucleation present above as well as inside the forest,
- no positive ion-induced nucleation,
- negative ion-induced nucleation only inside the forest,
- size and density of non-evaporating growth units of the first condensing substance: 0.55 nm and 2 $\mathrm{g\ cm^{-3}}$,
- effective dipole polarizability: 0.149 $\mathrm{nm^3}$,
- the plain Knudsen growth rate: 2 $\mathrm{nm\ h^{-1}}$,
- critical size and extra temperature of quantum rebound: 2.5 nm and 600 K,
- size of growth units of second condensing substance: 0.8 nm,
- the plain Knudsen growth rate: 5 $\mathrm{nm\ h^{-1}}$,
- the nano-Köhler threshold diameter: 3 nm,
- the power of the nano-Köhler approximation: 2,
- average diameter of background aerosol particles: 50 nm,
- average concentration of background aerosol particles: 3000 $\mathrm{cm^{-3}}$,
- wind speed in the forest: 1 $\mathrm{m\ s^{-1}}$,
- air residence time: 200 s,
- conifer needle diameter: 0.9 mm,
- total length of needles in a unit volume: 200 $\mathrm{m^{-2}}$.

The calculations were made with 3600 time

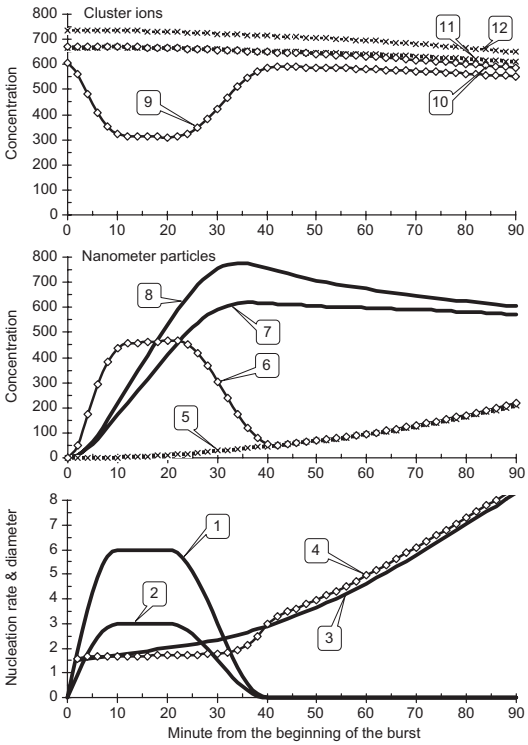


**Fig. 2**. Simulated instance of a fictitious nucleation burst. Neutral nucleation is expected above as well as inside of the forest canopy and negative ion-induced nucleation is expected only inside the canopy. Details of the conditions are explained in the text. Curves: 1: nucleation rate of neutral particles above and inside the canopy ($cm^{-3}$ $s^{-1}$), 2: nucleation rate of negative particles, only inside the canopy ($cm^{-3}$ $s^{-1}$), 3: average diameter of neutral nanometer particles inside the canopy (nm), 4: average diameter of negative nanometer particles inside the canopy (nm), 5: concentration of positive nanometer particles inside the canopy ($cm^{-3}$), 6: concentration of negative nanometer particles inside the canopy ($cm^{-3}$), 7: concentration of neutral nanometer particles inside the canopy (10 $cm^{-3}$), 8: concentration of neutral nanometer particles above the canopy (10 $cm^{-3}$), 9: concentration of negative cluster ions inside the canopy ($cm^{-3}$), 10: concentration of negative cluster ions above the canopy ($cm^{-3}$), 11: concentration of positive cluster ions inside the canopy ($cm^{-3}$), 12: concentration of positive cluster ions above the canopy ($cm^{-3}$).

steps and 2997 size sections up to diameter of 11.8 nm.

The nucleation burst lasts for 40 minutes and remains at the peak value during 10 minutes (curves 1 and 2 in Fig. 2). There are no nanometer particles in the air before the burst and the concentrations of cluster ions stay at the steady-state values. The concentration of negative ions is less than the concentration of positive ions due to their higher mobility, which results in their enhanced adsorption by background aerosol particles and conifer needles. While larger ionization rates inside the forest canopy increases the ion concentration there, adsorption of ions onto needles decreases it. The effect of needles dominates in the example, so the concentrations of ions inside of the forest canopy are smaller than above the forest (compare curves 9–12 in Fig. 2). This is characteristic of the present fictitious example and the proportions of ion concentrations above and inside of the forest can be opposite in real situations (Tammet *et al.* 2006). The concentration of negative cluster ions inside of the canopy has a deep depression (curve 9 in Fig. 2) during the nucleation burst due to the loss of ions transforming into particles, which happens in the example only with negative ions inside of the canopy. This kind of depression can be considered as a sensitive indicator of the ion-induced nucleation when analyzing real measurements.

The concentrations of neutral and charged nanometer particles are illustrated with curves 5–8 in Fig. 2. The concentrations of neutral particles essentially exceed the concentrations of charged particles, even though the intensity of ion-induced nucleation is relatively high in the example (note that the unit of curves 7 and 8 is 10 $cm^{-3}$ compared with 1 $cm^{-3}$ of curves 5 and 6). The reason is the short life time of charged particles within a few minutes due to their neutralization by cluster ions of opposite polarity. There is no positive ion-induced nucleation in the example, so the positive charged particles appear as a result of a diffusion combination of neutral particles with positive ions. When the negative ion-induced nucleation deceases, the concentrations of negative and positive charged particles become nearly equal. The continued increase in the concentration of charged particles after the end of the burst is explained by the growth of neutral particles and accompanied by an increase in the charging probability. The concentration of nanometer particles inside of the forest is slightly suppressed by the adsorption of finest particles onto the conifer needles. This is a direct analogue of the effect of the adsorption of fresh

nuclei onto large aerosol particles described by Kerminen and Kulmala (2002).

The growth of the average diameter of particles is illustrated with curves 3 and 4 in Fig. 2. The growth is accelerated after passing the nano-Köhler threshold diameter, which is assumed to be 3 nm in the example. The average diameter of negative particles remains less than the average diameter of neutral particles during the burst because most of the fresh negative particles are neutralized before they manage to grow. After the burst, the situation changes to opposite and negative particles are bigger because now they are born as a result of diffusion charging and the charging probability increases with particle size.

## Summary

The model described in the present paper is an extension to the model published previously by Tammet and Kulmala (2005). The model can be used to fit aerosol and ion data and to interpret nucleation bursts taking place in a coniferous forest. The 95 input parameters of the model can be adjusted by the user by editing an input file.

The equation of the evolution and balance of small ions includes the suppression of ion concentration by ion-induced nucleation, the effect of asymmetric charge of aerosol particles, and dry deposition of ions onto the forest canopy. The dry deposition is calculated using the Churchill-Bernstein heat transfer equation, translated to the terms of the particle diffusion as proposed by Tammet *et al*. (2001, 2006). The factor of depletion of ions onto large particles of the pre-existing aerosol is parameterized and the size distribution of these particles is represented with their concentration and average size.

It is expected that the units attaching to growing particles may be, in addition to small inorganic molecules, clusters of molecules or large organic molecules. Thus the size of the growth units is not neglected and the condensation is considered as the coagulation of growth units with the growing particle. Two kinds of the growth units with different sizes and parameters are simultaneously considered in the model. The combination of ions and particles and the growth of particles are modeled according to algorithms explained by Tammet and Kulmala (2005).

The computing time for an ordinary PC is counted in seconds in case of a typical task with several thousands of time steps and several thousands of size sections. The huge number of size sections suppresses the effect of the numerical diffusion. The flexibility, convenient control of input parameters and computing efficiency make the simulator a useful tool in looking for the interpretation of measurements of atmospheric aerosol nucleation bursts. The presented numeric example shows that dry deposition onto the canopy plays a considerable role in the development of nucleation bursts inside a forest.

*Acknowledgements*: This work was supported by the Estonian Science Foundation under grant no. 6226. The authors thank Dr. M. Noppel, Dr. J. Salm, and Dr. U. Hõrrak for valuable discussions.

## References

Chen J.M., Rich P.M., Gower S.T., Norman J.M. & Plummer S. 1997. Leaf area index of boreal forests: theory, techniques, and measurements. *J. Geophys. Res.* 102: 29429–29443.

Dal Maso M., Kulmala M., Riipinen I., Wagner R., Hussein T., Aalto P.P. & Lehtinen K.E.J. 2005. Formation and growth of fresh atmospheric aerosols: eight years of aerosol size distribution data from SMEAR II, Hyytiälä, Finland. *Boreal Env. Res.* 10: 323–336.

Fuchs N.A. & Sutugin A.G. 1971. High-dispersed aerosols. In: Hidy G.M & Brock J.R. (eds.), *Topics in current aerosol research*, Pergamon Press, pp. 1–60.

Hoppel W.A. & Frick G.M. 1986. Ion-aerosol attachment coefficients and steady-state charge distribution on aerosols in a bipolar ion environment. *Aerosol Sci. Technol.* 5: 1–21.

Incropera F.P. & Dewitt, D.P. 2002. *Fundamentals of heat and mass transfer*. Wiley, New York.

Kerminen V.-M. & Kulmala M. 2002. Analytical formulae connecting the "real" and the "apparent" nucleation rate and the nuclei number concentration for atmospheric nucleation events. *J. Aerosol Sci.* 33: 609–622.

Kulmala M., Pirjola L. & Mäkelä J. M. 2000. Stable sulphate clusters as a source of new atmospheric particles. *Nature* 404: 66–69.

Kulmala M., Kerminen V.-M., Anttila T., Laaksonen A. & O'Dowd C.D. 2004a. Organic aerosol formation via sulphate cluster activation. *J. Geophys. Res.* 109, D04205, doi:10.1029/2003JD003961.

Kulmala M., Vehkamäki H., Petäjä T., Dal Maso M., Lauri A., Kerminen V.-M., Birmili W. & McMurry P.H. 2004b. Formation and growth rates of ultrafine atmospheric particles: A review of observations. *J. Aerosol Sci.* 35:

143–176.

Nadykto A.B. & Yu F. 2003. Uptake of neutral polar vapor molecules by charged clusters/particles: Enhancement due to the dipole-charge interaction. *J. Geophys. Res.* 108(D23), 4717, doi:10.1029/2003JD003664.

Rannik Ü., Aalto P., Keronen P., Vesala T. & Kulmala M. 2003. Interpretation of aerosol particle fluxes over a pine forest: Dry deposition and random errors. *J. Geophys. Res.* 108(D17), 4544. doi:10.1029/2003JD003542.

Reischl G.P., Mäkelä J.M., Karch R. & Necid J. 1996. Bipolar charging of ultrafine particles in the size range below 10 nm. *J. Aerosol Sci.* 27: 931–949.

Seinfeld J.H. & Pandis S.N. 1998. *Atmospheric chemistry and physics: from air pollution to climate change*. John-Wiley & Sons, New York.

Tammet H. 1995. Size and mobility of nanometer particles, clusters and ions. *J. Aerosol Sci.* 26: 459–475.

Tammet H. & Kulmala M. 2005. Simulation tool for atmospheric aerosol nucleation bursts. *J. Aerosol Sci.* 36: 173–196.

Tammet H., Kimmel V. & Israelsson S. 2001. Effect of atmospheric electricity on dry deposition of airborne particles from atmosphere. *Atmos. Environ.* 35: 3413–3419.

Tammet H., Hõrrak U., Laakso L. & Kulmala M. 2006. Factors of air ion balance in a coniferous forest according to measurements in Hyytiälä, Finland. *Atmos. Chem. Phys.* 6: 3377–3390.

Wesely M.L. & Hicks B.B. 2000. A review of the current status of knowledge on dry deposition. *Atmos. Environ.* 34: 2261–2282.